CLM - P 693

CLM - P 693

UKAEA

Preprint

THE EFFECT OF A RELATIVISTIC RESONANCE CONDITION ON THE FOKKER-PLANCK THEORY OF ECRH CURRENT DRIVE

D. F. H. START
M. R. O'BRIEN
P. M. V. GRACE

CULHAM LABORATORY
Abingdon Oxfordshire
1983

CLM-P693

THE EFFECT OF A RELATIVISTIC RESONANCE CONDITION ON THE FOKKER-PLANCK THEORY OF ECRH CURRENT DRIVE

D F H Start, M R O'Brien and P M V Grace*
Culham Laboratory, Abingdon, Oxon, OX14 3DB, UK
(Euratom/UKAEA Fusion Association)
*St John's College, Cambridge, UK.

ABSTRACT

The efficiency of current drive by X-mode electron cyclotron waves is calculated using the weakly relativistic resonance condition in a full Fokker-Planck treatment which includes electron-electron collisions. For suprathermal resonant electrons the values obtained are less by a factor (Z+5)/Z than those predicted by the Lorentz gas model. However this relationship is found not to hold for resonant parallel velocities less than the thermal velocity. A ray tracing code, incorporating the calculated current drive efficiencies, has been used to study the relativisitic corrections for X-mode second harmonic waves injected from the low field side into a tokamak the size of DITE.

(Submitted for publication in Plasma Physics)

May 1983

1 INTRODUCTION

The non-inductive current drive scheme using electron cyclotron resonance heating (ECRH) relies on preferentially heating electrons which are moving in one direction along the magnetic field lines [1]. This can be achieved by tuning the wave frequency ω such that the Doppler shift due to the electron velocity along the magnetic field synchronises the wave frequency and the electron gyrofrequency or one of its harmonics. Thus for non-relativistic electrons, resonance is achieved for all perpendicular velocities provided the parallel velocity $v_\parallel$ satisfies the condition $(\omega-\ell\Omega) = k_\parallel v_\parallel$, where $k_\parallel$ is the parallel wave vector, Ω is the electron gyrofrequency and ℓ is the harmonic number. Electrons moving parallel (antiparallel) with the wave will be in resonance if the wave frequency is greater (less) than $\ell\Omega$. In the inhomogeneous field of a tokamak the frequency difference $(\omega-\ell\Omega)$ changes sign across the resonance layer so that the current flows in opposite directions on opposite sides of the resonance. For a weakly absorbed wave these opposing currents are of equal amplitude and no net current flows.

As the electrons become relativistic the gyrofrequency develops a velocity dependence due to the relativistic mass increase. This velocity dependence can affect both the absorption profiles[2 3] and, as shown in a recent paper by Cairns, Owen and Lashmore-Davies[4], can substantially change and enrich the phenomenology of ECRH current drive. The principal effect is that the current is no longer an antisymmetric function of $(\omega-\ell\Omega)$ where Ω is the non-relativistic gyrofrequency. Thus in a tokamak the currents on opposite sides of the cyclotron resonance layer have different amplitudes and do not cancel in the case of weak absorption.

The calculations in ref 4 used a simplified collision operator which neglected electron-electron collisions. In the present paper we include these collisions in a full Fokker-Planck treatment for X-mode cyclotron waves of arbitrary harmonic number ℓ. The results have been incorporated into a ray tracing code which is used to compare the relativistic and non-relativistic calculations in a practical application. For this we have chosen the example of second harmonic X-mode RF injected into a tokamak similar to DITE.

2 THE RESONANCE CONDITION

The electron cyclotron resonance condition for mildly relativistic electrons can be written

$$k_\parallel v_\parallel = \omega - \ell\Omega \left(1 - \frac{v_\parallel^2+v_\perp^2}{2c^2}\right) \qquad (1)$$

where c is the velocity of light and $v_\parallel$ and $v_\perp$ are the electron parallel and perpendicular velocities respectively. In terms of normalised velocity space co-ordinates, $v_\parallel/v_e$ and $v_\perp/v_e$, the resonance condition is a semicircle of radius $(1-4u_oS)^{\frac{1}{2}}/2S$ centred on the $v_\perp/v_e=0$ axis at $v_\parallel/v_e = (2S)^{-1}$. The parameters u_o and S are defined by $u_o=(\omega-\ell\Omega)/k_\parallel v_e$ and

$S=\ell\Omega v_e/(2k_\parallel c^2)$ and the electron thermal velocity, v_e, is related to the temperature, T_e, by $v_e^2 = 2T_e/m$, where m is the electron mass. In the non-relativistic limit the resonance becomes the straight line $v_\parallel/v_e = u_o$. Several resonance curves for positive values of S are shown in Fig 1 for both $u_o = 1$ and $u_o = -1$. For $S > 0$, positive values of u_o correspond to absorption on the low field side of the ECR in a tokamak. In this case the mass increase serves to increase the difference between the wave frequency and the gyrofrequency leading to resonant values of $v_\parallel$ which are always positive and greater than the non-relativistic value. Note that for $S > (4u_o)^{-1}$ the frequency difference cannot be recovered by the Doppler shift for any value of $v_\parallel$ and so a cut-off in the wave absorption occurs. At cut-off the resonance semi-circle collapses to a point at $v_\parallel/v_e = 2u_o$, $v_\perp/v_e = 0$.

On the high field side of the ECR the gyrofrequency exceeds the wave frequency for non-relativistic electrons and the resonance condition is satisfied by negative values of $v_\parallel$. However for sufficiently energetic electrons the mass increase causes the gyrofrequency to fall below the wave frequency giving rise to positive values of $v_\parallel$ at resonance as shown in Fig 1. Thus on the high field side electrons moving both parallel and antiparallel to the wave can absorb power. For propagation of the wave perpendicular to the magnetic field ($k_\parallel = 0$) all directionality disappears as expected and the wave is absorbed by iso-energetic electrons. The resonance curve is the zero-centred semicircle given by $v^2 = 2(\ell\Omega - \omega)c^2/(\ell\Omega)$.

3 THE FOKKER-PLANCK EQUATION

The linearised, steady state electron Fokker-Planck equation can be written as [5]

$$\frac{1}{v_\perp}\frac{\partial}{\partial v_\perp}\left\{ D v_\perp \left(\frac{v_\perp}{v_e}\right)^{2(\ell-1)} \delta\left[\frac{\omega}{k_\parallel} - \frac{\ell\Omega}{k_\parallel}\left(1 - \frac{v^2}{2c^2}\right) - v_\parallel\right]\frac{\partial F_{me}}{\partial v_\perp}\right\} \qquad (2)$$

$$+ C_{ei}(f_e', F_{mi}) + C_{ee}(f_e', F_{me}) + C_{ee}(F_{me}, f_e') = 0$$

where the first term is the quasi-linear diffusion operator describing the effect of X-mode wave absorption, C represents the non-relativistic Fokker-Planck collision operator, and f_e' is the perturbation of the electron distribution function away from the Maxwellian F_{me}. The parameter D for the X-mode is independent of velocity space variables and is proportional to the square of the perpendicular electric field component which rotates in phase with the electrons. Using the Legendre polynomial representation of f_e', namely $f_e' = F_{me}\Sigma a_n P_n(v_\parallel/v)$, we find that the coefficient a_1, from which the current can be calculated, satisfies the integro-differential equation

$$a_1'' + P(x)\, a_1' + Q(x)\, a_1 - \frac{16}{3\pi^{\frac{1}{2}}\Lambda}\left[xI_3(x)-1.2xI_5(x)-x^4(1-1.2x^2)(I_o(x)-I_o(\infty))\right] = R(x) \tag{3}$$

where the dash denotes differentiation with respect to $x(=v/v_e)$. The terms on the left hand side are due entirely to the collisions while the term on the right hand side is due to the wave interaction and is given by

$$R(x) = \frac{12D}{v_e^3 \nu_o \Lambda}(x^2-x_o^2)^{\ell-1} x_o x\{x_o^2 + \ell - x^2 + [x^2-(2\ell+1)x_o^2]Sx_o^{-1}\}\{H(x-\alpha_-)-H(x-\alpha_+)\} \tag{4}$$

where $\alpha_\pm = \left|(1\pm\sqrt{1-4u_oS})/2S\right|$, $x_o=u_o+x^2S$, $\nu_o=e^4 n_e \ell n\lambda/4\pi\varepsilon_o^2 v_e^3 m^2$, $\Lambda=E-xE'$, H is the Heaviside function, n_e is the electron density, $\ell n\lambda$ is the Coulomb logarithm and E is the error function. In eqn (3) the functions P(x), Q(x) and $I_n(x)$ are those defined in ref 5, namely

$$P(x) = -x^{-1}-2x+2x^2E'/\Lambda \tag{5}$$

$$Q(x) = x^{-2}-2(Z+E-2x^3E')/\Lambda \tag{6}$$

$$I_n(x) = \int_o^x a_1(y)e^{-y^2}y^n dy \tag{7}$$

where Z is the effective plasma charge.

Note that a change of sign of $k_\parallel$ simultaneously reverses the signs of both u_o and S thereby changing the sign but not the magnitude of R(x). Physically this means that for a wave propagating through a tokamak plasma a reversal of the wave direction reverses the currents on each side of the resonance but leaves their magnitudes unchanged. Thus in the following calculations we shall keep $k_\parallel$ positive (S positive) and change the sign of u_o to investigate the low and high field sides of the resonance.

The electron current density J is given by

$$J = -e\int v_\parallel f_e' d^3v = -\frac{4e}{3\pi^{\frac{1}{2}}} v_e n_e I_3(\infty) \tag{8}$$

and the absorbed power density by

$$P_d = \tfrac{1}{2}m_e\int \frac{v^2}{v_\perp}\frac{\partial}{\partial v_\perp}\left\{Dv_\perp\left(\frac{v_\perp}{v_e}\right)^{2(\ell-1)}\delta\left[\frac{\omega}{k_\parallel}-\frac{\ell\Omega}{k_\parallel}\left(1-\frac{v^2}{2c^2}\right)-v_\parallel\right]\frac{\partial F_{me}}{\partial v_\perp}\right\}d^3v \tag{9}$$

Changing variables to x and $\xi = (v_\parallel/v)$ and integrating we obtain

$$P_d = 4Dn_e m_e G_\ell/(\pi^{\frac{1}{2}} v_e) \tag{10}$$

where $$G_\ell = \int_{\alpha_-}^{\alpha_+} x^3(x^2-x_o^2)^{\ell-1}(x^2-x_o^2-\ell+2\ell x_o S)e^{-x^2}dx \tag{11}$$

Expressions for G_ℓ are given in the appendix for $\ell = 1$ and $\ell = 2$. In the usual units of $-nev_e$ for J and $nm_e v_e^2 \nu_o$ for P_d, the current drive efficiency J/P_d is given by

$$\frac{J}{P_d} = \frac{v_e^3 \nu_o}{3D} \cdot \frac{I_3(\infty)}{G_\ell} \tag{12}$$

4. LORENTZ GAS SOLUTION

If electron-electron collisions can be neglected in comparison with the electron-ion collisions, as is the case for large values of the plasma ionic charge, then an analytic solution of eq(3) can be obtained;

$$a_1 = -\frac{6D}{v_e^3 \nu_o Z}(x^2-x_o^2)^{\ell-1} x_o x \{x_o^2+\ell-x^2+[x^2-(2\ell+1)x_o^2]Sx_o^{-1}\}\{H(x-\alpha_-)-H(x-\alpha_+)\} \tag{13}$$

The current drive efficiency is given by

$$\frac{J}{P_d} = -\frac{2}{G_1 Z}\int_{\alpha_-}^{\alpha_+} x_o x^4(x^2-x_o^2)^{\ell-1}\{x_o^2+\ell-x^2+[x^2-(2\ell+1)x_o^2]Sx_o^{-1}\}e^{-x^2}dx \tag{14}$$

For $\ell=1$ this becomes

$$\frac{J}{P_d} = -\frac{2}{G_1 Z}\left[AJ_4 + BJ_6 + CJ_8 + S^3 J_{10}\right] \tag{15}$$

where $$J_n = \int_{\alpha_-}^{\alpha_+} x^n e^{-x^2}dx, \tag{16}$$

$$A = u_o^3+u_o-3Su_o^2 , \tag{17}$$

$$B = 3u_o^2 S-u_o+2S-6u_o S^2 \tag{18}$$

$$C = S(3u_o S-1-3S^2) \tag{19}$$

and G_1 is given by eq(A2) in the appendix. Values of J/P_d derived from eq(15) and multiplied by the factor $Z(Z+5)^{-1}$ (see Section 5) are plotted as a function of S for various values of u_o in Fig. 2. The current drive efficiencies obtained from the numerical solution of the full equation are also shown for comparison.

5. NUMERICAL SOLUTION

Equation (3) has been solved numerically using the two point boundary value code described by Cordey et al [6]. The discontinuities in R(x) at x =

α_- and $x = \alpha_+$ were smoothed as described in ref 6. Values of J/P_d were obtained for values $-3<u_o<3$, $0<S<2$, $Z = 1,2$ and harmonic numbers $\ell=1$ and $\ell=2$. Efficiencies for the fundamental frequency are listed in Table 1. More extensive tables for both X-mode and O-mode and for $\ell=1$ and $\ell=2$ are given in ref 7. Curves of J/P_d for the fundamental frequency are plotted against S in Fig. 2 for $u_o = 0.1$, 0.5, 1 and 3 respectively. As S increases from zero, the efficiency on the low field side increases dramatically whereas that on the high field side is reduced. For sufficiently large values of S the current on the high field side reverses although this occurs more readily for the lower values of u_o. This reversal takes place because the relativistic mass increase takes the gyrofrequency from above to below the wave frequency.

The dashed curves show the Lorentz gas results multiplied by the factor $Z(Z+5)^{-1}$ which relates the results of the full numerical calculation to the Lorentz values for $u_o>3$ in the non-relativistic case[1]. According to Cairns et al [4] this ratio should be maintained in the mildly relativistic case. This is indeed correct as is shown in Fig. 2 by the steadily improving agreement between the two calculations as u_o is increased. For $u_o=3$ the agreement is essentially complete, at least for values of S up to 0.5. However there are large differences between the numerical and renormalised Lorentz results, in both the relativistic and non-relativistic cases, for velocities $u_o< 1$ which are likely to be appropriate to near term experiments. The present non-relativistic numerical results agree well with those of Karney and Fisch[8] when these authors model the complete electron-electron collison operator through the use of a displaced Maxwellian background electron distribution.

In Fig.3 the efficiency, current and absorbed power for the $\ell=2$ case are plotted as a function of u_o for S = 0.06 and S = 0.24 and show the asymmetry about $u_o=0(\omega=\ell\Omega)$ which develops as the relativistic effects become significant.

6 RAY TRACING CALCULATIONS

In order to predict the effect of the relativistic resonance condition in a tokamak experiment, the results of the Fokker-Planck calculation have been incorporated into a ray tracing code. Ray tracing using the cold plasma dispersion relation has been discussed by, for example, Fidone et al[3] and Ott et al[9]. The present code uses the weakly relativistic expression for the dielectric tensor given by Shkarofsky[10] from which the absorption coefficient is obtained as described by Bornatici[11]. The power absorbed and the values of u_o and S were calculated at each point along the ray. The results obtained in the previous section for J/P_d were then used to obtain the current density profile.

Typical ray paths for X-mode, 60 GHz second harmonic electron cyclotron waves injected from the low field side into a tokamak of similar

size to DITE are shown in Fig 4. The major radius (R) was 1.17 m and the minor radius (a) was 0.26m. Plasma temperature and density profiles were taken to be parabolic in form, $T_e(r) = T_{eo}[1-(r/a)^2]$ and $n_e(r) = n_{eo}[1-(r/a)^2]$ with central values T_{eo} = 1keV and $n_{eo} = 10^{13}cm^{-3}$. The resonance surface $2\Omega = \omega$ passed through the magnetic axis and the rays were injected on the mid-plane at different angles ψ $(\simeq \tan^{-1}(k_{\parallel}/k_r))$ to the major radius. The total current obtained as a function of ψ is shown in Fig.5 for both the relativistic and non-relativistic calculations. In both cases more than 95% of the input power was absorbed for $\psi < 30°$. The major difference in the two curves appears at low values of ψ (small $k_{\parallel}$, large S) where the rapid drop in current predicted by the relativistic theory contrasts with the almost constant current given by the non-relativistic calculation. For these small values of $k_{\parallel}$ the Doppler shift component in the resonance condition plays only a minor role compared with the mass increase. Resonance is then determined largely by the energy, rather than the parallel velocity, of an electron and the current drive efficiency correspondingly falls. The discontinuity in current occurring at $\psi = 35°$ corresponds to the transition from a ray hitting the inside wall (case A) to one making a double pass through the resonance region (case B). For large angles the rays are unable to reach this region (case C). In addition the relativistic cut-off on the low field side operates to reduce the current generated by such rays.

From Fig.5 it can be seen that to sustain a plasma current of 100 kA would require 1.5 MW of ECRH power. On the basis of a calculation akin to that of Fielding[12] we find that, for this amount of power, the quasi-linear diffusion coefficient is still substantially less than that due to collisions so that our perturbation treatment remains valid.

In higher temperature tokamaks the relativistic effects will not be restricted to quasi-perpendicular propagation. For example, in the non-relativistic calculations of Edlington et al[13], for X-mode fundamental waves injected from the high field side into a JET-sized tokamak, a typical value of S is 0.2 for T_{eo}=10 keV and $N_{\parallel}=0.6(N_{\parallel}=k_{\parallel}c/\omega)$. The effective value of u_o was approximately three and so from Fig.2 one might expect a 30% reduction in the predicted current drive efficiency if the relativistic resonance condition were to be incorporated into these calculations.

7 SUMMARY

A full Fokker-Planck treatment of current drive by ECRH has been carried out with relativistic corrections applied to the resonance condition. The results are expressed in terms of u_o, which is the parallel velocity (normalised to v_e) of the resonant electrons in the non-relativistic case, and S which parameterises the relativistic effect. In this form the results can be readily incorporated into ray tracing codes. For $u_o > 3$ the values of J/P_d were found to be in good agreement with those obtained from a Lorentz gas model (electron-electron collisions neglected)

when the latter were multiplied by $Z(Z+5)^{-1}$ as suggested by Cairns et al [4]. However, for smaller values of u_o the renormalised Lorentz gas model substantially underestimates the current drive efficiency for almost all values of S. Ray tracing calculations for the example of second harmonic X-mode radiation strongly absorbed in a tokamak similar to DITE show a reduction in current drive efficiency as relativistic effects become important. This is expected to be a feature of all ECRH current drive schemes since it is due to the resonance condition becoming dominated by the energy dependent mass increase rather than the parallel velocity dependent Doppler shift.

Acknowledgements

We wish to thank J A Owen for the use of his code to calculate the relativistic dielectric tensor used in the ray tracing calculations.

REFERENCES

1 N J Fisch and A H Boozer, Phys Rev Lett, 45 (1980) 720.
2 I Fidone, G Granata and R L Meyer, Plasma Physics 22 (1980) 261
3 I Fidone, G Granata and R L Meyer, Phys.Fluids 25 (1982) 2249
4 R A Cairns, J Owen and C N Lashmore-Davies to be published in Phys. Fluids.
5 J G Cordey, T Edlington and D F H Start, Plasma Physics 24 (1982) 73.
6 J G Cordey et al, Nuclear Fusion 19 (1979) 249
7 D F H Start, M R O'Brien and P M V Grace, Culham Laboratory report CLM-R240 (1983).
8 C F F Karney and N J Fisch, Nuclear Fusion 21 (1981) 1549.
9 E Ott, B Hui and K R Chu, Phys.Fluids 23 (1980) 1031
10 I P Shkarofsky, Phys Fluids, 9(1966) 561
11 M Bornatici, Proc of Joint Workshop on Electron Cyclotron Emission Electron Cyclotron Resonance Heating, Oxford, July 1980, Culham Laboratory Report (CLM-EMR(1980)).
12 P J Fielding, Proc. Joint Workshop on Electron Cyclotron Emission and Electron Cyclotron Resonance Heating, Oxford, July 1980, Culham Laboratory Report (CLM-EMR(1980)).
13 T Edlington, J G Cordey, M O'Brien and D F H Start, Proc. 3rd Joint Varenna-Grenoble Int. Symp on Heating in Toroidal Plasmas 3 869, Grenoble 1982.

APPENDIX

The expression for the power density, eq(10), contains the integral G_ℓ defined by

$$G_\ell = \int_{\alpha_-}^{\alpha_+} x^3 (x^2-x_o^2)^{\ell-1} [x^2-x_o^2-\ell+2\ell x_o S] e^{-x^2} dx \tag{A1}$$

Evaluating this integral for $\ell=1$ gives

$$G_1 = \frac{1}{2}[-S^2K_3+(1-2u_oS+2S^2)K_2 - (1+u_o^2-2u_oS)K_1] \tag{A2}$$

where $K_n = \int_a^b y^n e^{-y} dy$, $a=\alpha_-^2$ and $b = \alpha_+^2$

The integrals K_n can be obtained from the recurrence relation:

$$K_n = nK_{n-1} + a^n e^{-a} - b^n e^{-b} \tag{A3}$$

Similarly for $\ell=2$ we find

$$\begin{aligned} G_2 = \frac{1}{2}[& S^4K_5-2S^2(1-2u_oS+2S^2)K_4 \\ & + (1-4u_oS+6S^2+6u_o^2S^2-12u_oS^3)K_3 \\ & - 2(1+u_o^2-4u_oS-2u_o^3S+6u_o^2S^2)K_2 \\ & + u_o^2(2+u_o^2-4u_oS)K_1] \end{aligned} \tag{A4}$$

TABLE 1 VALUES OF J/P_d FOR $\ell=1$ and $Z=1$

S	$U_o = -2.0$	-1.0	-0.5	-0.1	0.1	0.5	1.0	2.0
0.0	-2.87	-1.45	-0.82	-0.18	0.18	0.82	1.45	2.87
0.02	-2.68	-1.37	-0.76	-0.12	0.24	0.89	1.54	3.09
0.04	-2.51	-1.29	-0.69	-0.06	0.30	0.96	1.62	3.36
0.08	-2.22	-1.14	-0.56	0.06	0.43	1.09	1.79	4.17
0.12	-1.98	-1.00	-0.43	0.18	0.55	1.22	1.98	6.66
0.16	-1.76	-0.86	-0.31	0.30	0.66	1.35	2.18	0.00
0.20	-1.57	-0.73	-0.19	0.41	0.78	1.48	2.41	0.00
0.24	-1.39	-0.60	-0.08	0.52	0.88	1.59	2.66	0.00
0.3	-1.15	-0.43	0.08	0.66	1.02	1.73	0.00	0.00
0.6	-0.34	0.15	0.51	0.98	1.31	0.00	0.00	0.00
1.0	0.05	0.34	0.60	1.03	1.42	0.00	0.00	0.00
1.5	0.16	0.37	0.60	1.01	1.43	0.00	0.00	0.00
2.0	0.20	0.37	0.57	0.95	1.32	0.00	0.00	0.00

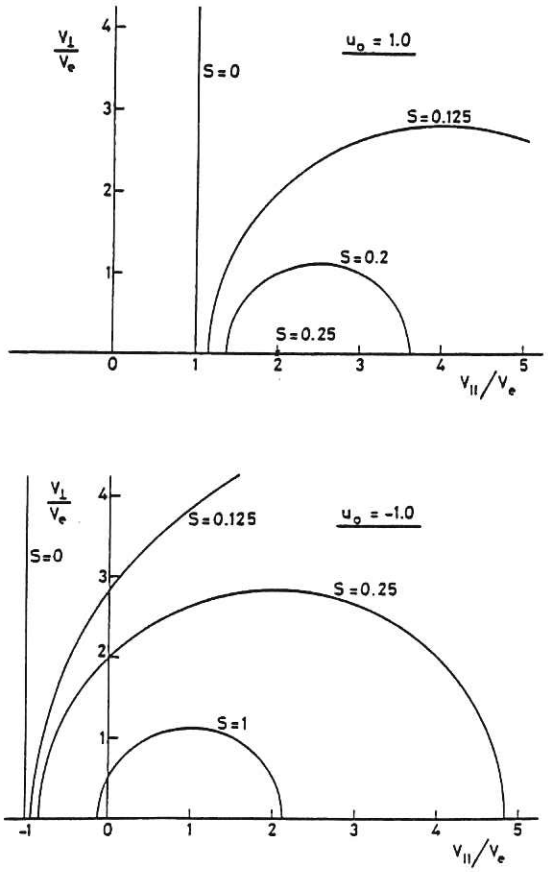

Fig.1 Electron-cyclotron resonance lines in velocity space for $u_o = 1$ and $u_o = -1$ for several values of S which parameterises the relativistic effect. Note the cut-off for $u_o = 1$ as S reaches the value 0.25.

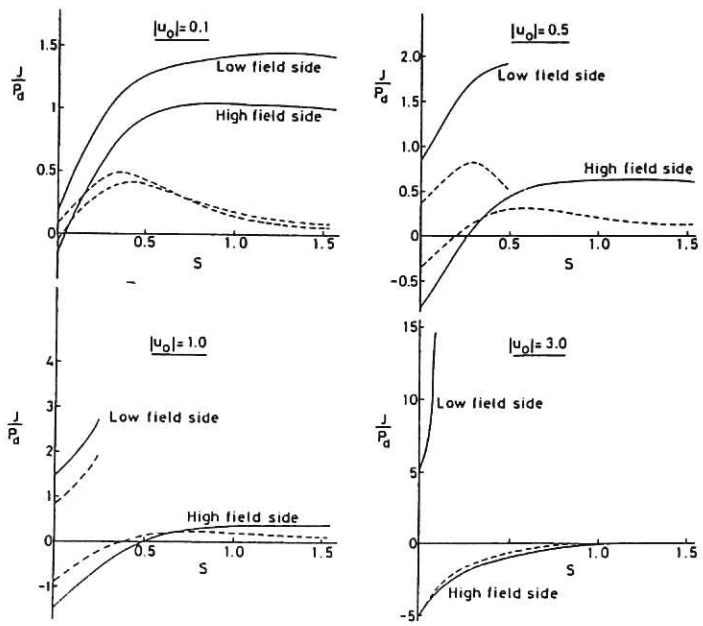

Fig.2 Current drive efficiency J/P_d versus S for $\ell = 1$ and $|u_o| = 0.1$, 0.5, 1 and 3. The curves labelled high (low) field side correspond to negative (positive) values of u_o. The cut-off on the low field side occurs for $S = (4u_o)^{-1}$. The dashed curves are the values obtained from the Lorentz gas model multiplied by $Z(Z+5)^{-1}$.

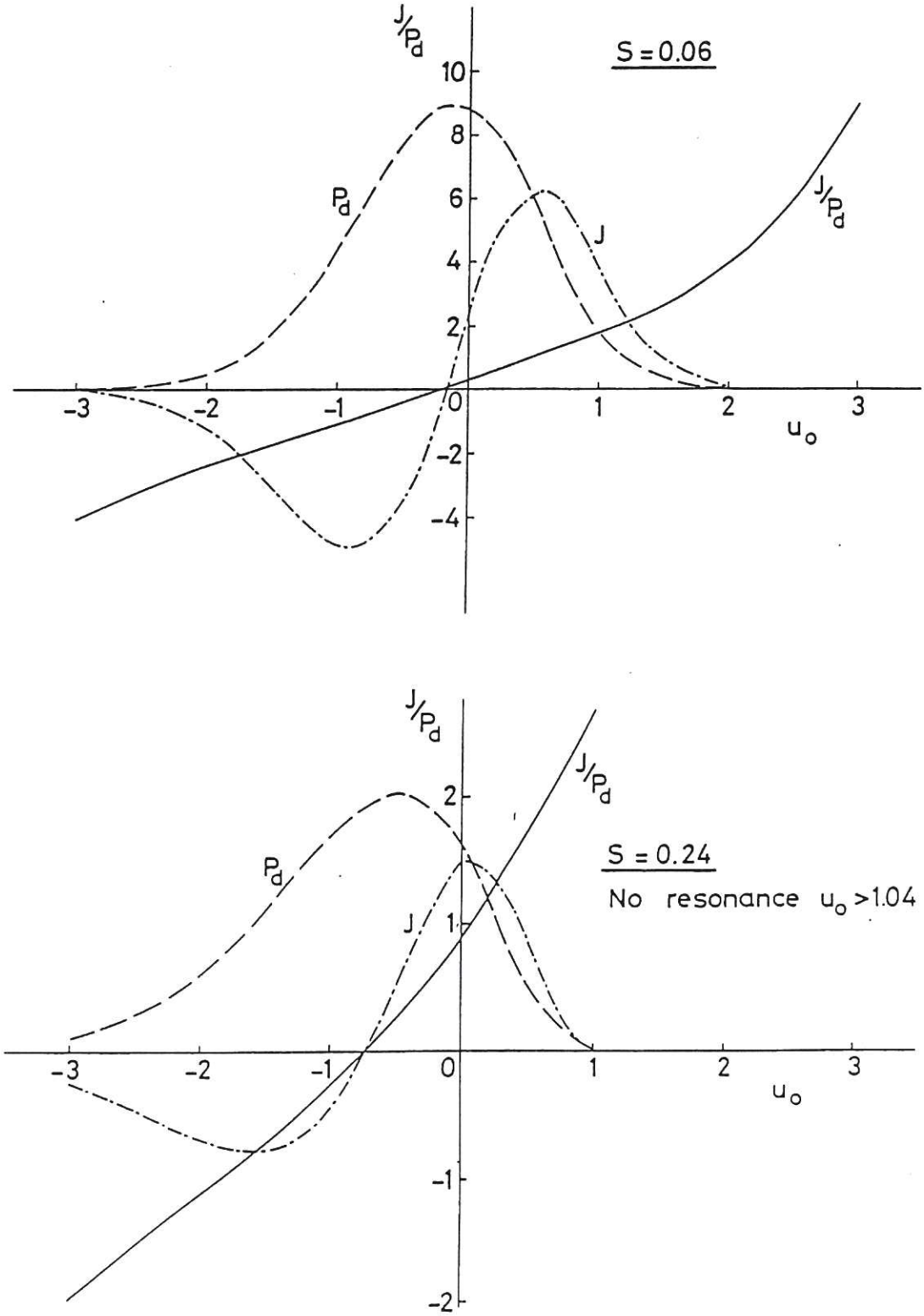

Fig.3 Curves of J/P_d, J and P_d versus u_o for $\ell = 2$ showing the loss of antisymmetry in the profiles as the value of S increases and relativistic effects become important. The power and current densities are expressed in arbitrary units. The cut-off on the low field side (positive u_o) occurs for $S = (4u_o)^{-1}$.

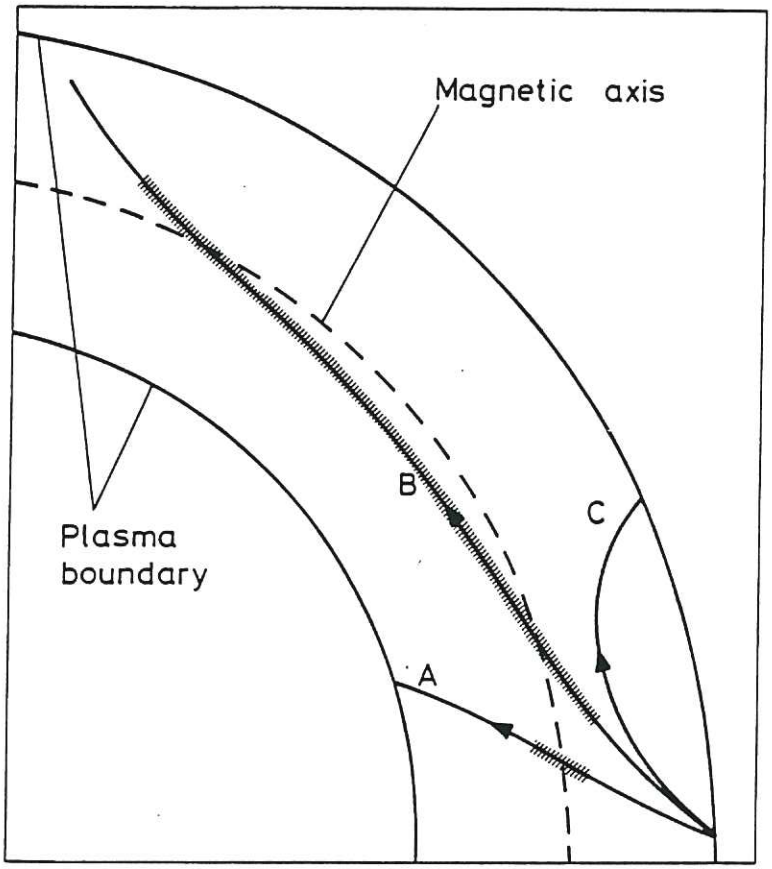

Fig.4 Plan view of ray paths for X-mode second harmonic cyclotron waves injected from the low field side into a tokamak with dimensions and plasma parameters similar to those of DITE. The rays A,B and C all originate in the median plane but at different angles ψ to the major radius.

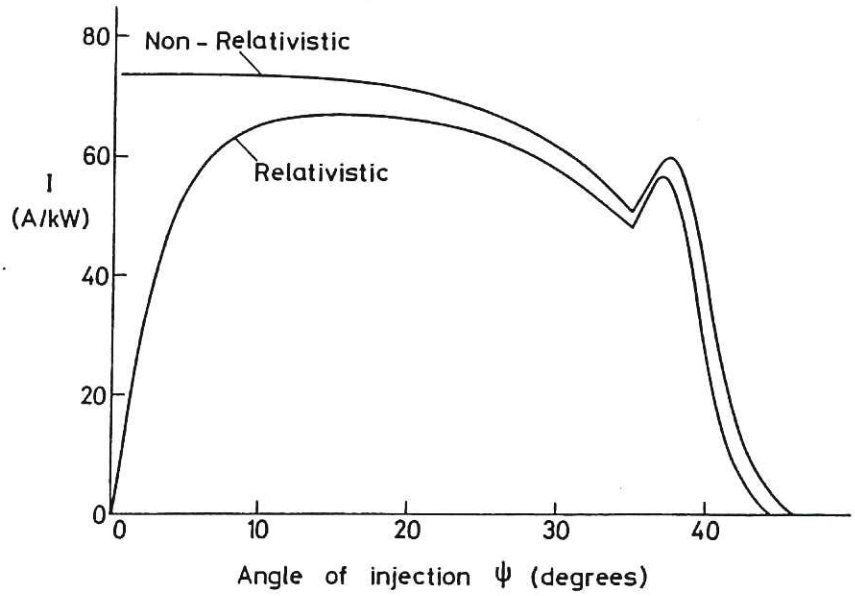

Fig.5 The current produced by rays such as those in Fig.4 versus the angle of injection to the major radius. Note the sharp reduction in current predicted by the relativistic calculation as the angle, and $k_{\parallel}$ become small.